Whole-Vehicle modelling of exhaust energy recovery on a diesel-electric hybrid bus

Briggs, I., McCullough, G., Spence, S., & Douglas, R. (2014). Whole-Vehicle modelling of exhaust energy recovery on a diesel-electric hybrid bus. *Energy*, *65*, 172-181. https://doi.org/10.1016/j.energy.2013.11.075

Published in:
Energy

Document Version:
Peer reviewed version

Queen's University Belfast - Research Portal:
Link to publication record in Queen's University Belfast Research Portal

Whole-Vehicle Modelling of Exhaust Energy Recovery on a Diesel-Electric Hybrid Bus

Ian Briggs*, Geoffrey McCullough, Stephen Spence, Roy Douglas

School of Mechanical & Aerospace Engineering
Queen's University Belfast
United Kingdom
BT9 5AH

Abstract

Hybrid vehicles can use energy storage systems to disconnect the engine from the driving wheels of the vehicle. This enables the engine to be run closer to its optimum operating condition, but fuel energy is still wasted through the exhaust system as heat. The use of a turbogenerator on the exhaust line addresses this problem by capturing some of the otherwise wasted heat and converting it into useful electrical energy.

This paper outlines the work undertaken to model the engine of a diesel-electric hybrid bus, coupled with a hybrid powertrain model which analysed the performance of a hybrid vehicle over a drive-cycle. The distribution of the turbogenerator power was analysed along with the effect on the fuel consumption of the bus. This showed that including the turbogenerator produced a 2.4% reduction in fuel consumption over a typical drive-cycle.

The hybrid bus generator was then optimised to improve the performance of the combined vehicle/engine package and the turbogenerator was then shown to offer a 3.0% reduction in fuel consumption. The financial benefits of using the turbogenerator were also considered in terms of fuel savings for operators. For an average bus, a turbogenerator could reduce fuel costs by around £1200 per year.

Keywords: diesel engine, turbogenerator, waste heat recovery, hybrid, bus

1. Introduction

This work studied the effect of waste energy recovery on a 2.4-litre diesel-electric hybrid bus. The aim of the work was to reduce the fuel consumption of the vehicle by using some of the wasted energy on the exhaust line to create useful electrical power for the vehicle. The work was driven by the global need to reduce consumption of fossil fuels as prices and demand continue to rise.

1.1. Automotive Industry

Within the automotive sector, emissions of toxic gases such as mono oxides of nitrogen (NO_X), hydrocarbons (HC), carbon monoxide (CO) and diesel particulate matter (PM) are closely regulated through schemes such as the European Emissions Standard [1]. However, greenhouse gases and fuel consumption are as yet unregulated in the UK, except through tax incentives for end-users who purchase more fuel-efficient vehicles. Within the USA, the CAFE regulations [2] do limit greenhouse gases but only for passenger cars and light trucks. Due to the pressure from market demand, manufacturers and operators are keen to reduce fuel consumption, and hence reduce greenhouse gases, in an attempt to minimise the impact of rising fuel prices.

Due to the inherent inefficiency of the internal combustion engine (ICE), a considerable amount of the fuel energy supplied to the engine is lost as waste heat in both the exhaust line and coolant system. Numerous technologies exist which could be used to recover this lost energy, some of which are described below.

*Corresponding author: Email: ibriggs02@qub.ac.uk, Tel: +44 (0) 28 9097 4569

1.1.1. Rankine Cycle

The Rankine Cycle has attracted a considerable amount of interest from automotive manufacturers such as BMW [3], with the turbosteamer concept, which aims to reduce fuel consumption through the use of a Rankine Cycle on the exhaust and coolant loops of the vehicle. Lopes et al. [4] provided an overview of the Organic Rankine Cycle (ORC) systems, and showed the possibilities of using the concept to recover waste heat, and Srinivasan et al. [5] tested an ORC on a diesel engine showing benefits to fuel efficiency and a reduction in emissions. However, whilst these papers prove it is possible to recover significant amounts of waste energy, the complexity of the system, along with the amount of equipment required to make the concept work, is considerable. Due to the size of equipment necessary (including, at minimum, heat exchangers, expander, condenser and pump), the concept may be attractive to the heavy truck industry, as reported in Nelson [6], which applied Rankine concepts to a 15-litre diesel engine. Although this paper envisioned recovering high amounts of power, the authors also uncovered several obstacles due to equipment size and the amount of pipework required for in-vehicle integration.

Domingues et al. [7] showed the potential of an ORC to recover waste heat from a 2.8-litre gasoline engine. The authors showed up to 3.5% using an optimised heat exchanger. The authors recognised the complexities of the system, which included low efficiency (the maximum reported system efficiency was 18%) and high operating pressure of the working fluid (up to 40bar for maximum efficiency).

1.1.2. Thermoelectric Power

A number of studies have also investigated the suitability of thermoelectric generators (TEGs) to recover waste heat. These devices use a temperature gradient to create electricity based on the Seebeck effect. Crane [8] suggested TEGs could be applied to a purpose-built radiator to recover heat from the coolant line. Modelling results show up to 2kW of energy could be recovered, but this required the engine to be operated aggressively, and is not necessarily representative of real-world driving conditions. Such a device is expensive, and the efficiency of the TEGs suffer from heat transfer effects on the vehicle's exhaust line.

Rowe [9] highlighted how existing materials are limited in their maximum operating temperature, which limits the automotive applications. Fairbanks [10] also showed how TEGs are better suited to low-power situations such as personal heating or cooling applications. Gou et al. [11] studied the potential for thermoelectric generators to recover waste heat from a radiator. A comprehensive modelling study showed that a TEG could recover a maximum power of 6W with a working temperature of just 90 ^{o}C. As this was applied to the coolant loop of a vehicle, the maximum temperature was therefore limited to this low value, which in turn limited the power produced from the device. The efficiency of the overall TEG system was also very low; generally the efficiency was below 0.5% in all simulations.

However, all these papers agreed that the power density of the commercially-viable TEGs is currently too low to have a serious benefit in the automotive environment. The maximum efficiency of the materials in these devices is approximately 5%, so further developments in thermoelectric material technology are required before they can recover a suitable amount of energy from the main sources of heat on the vehicle.

1.1.3. Turbomachinery

Turbocharging is intended to increase the volumetric efficiency of the engine. By charging the air on the intake stroke to higher than atmospheric pressure, an increased mass of air is drawn into the cylinder, which facilitates the injection of more fuel, thereby increasing power density. The turbocharger makes use of the exhaust gas which would otherwise be wasted at the end of the exhaust stroke of the piston, due to the geometrically given expansion ratio [12].

Turbocharging, in conjunction with engine downsizing, can also be used to provide the same amount of power from a smaller capacity engine, and due to the reduction in capacity, less fuel is required. Hence, turbocharging can be used to reduce fuel consumption.

The principle of turbocompounding extends this theory and places a second 'power' turbine on the exhaust line, usually downstream of the turbocharger turbine, linked to either a set of gears connected to the crankshaft (mechanical turbocompounding) or a small electric generator (turbogenerator). Alternatively, the turbocompound can take the form of a motor/generator on the shaft of the turbocharger (electric turbocharger). The three forms of turbo compounding are shown in Figure 1.

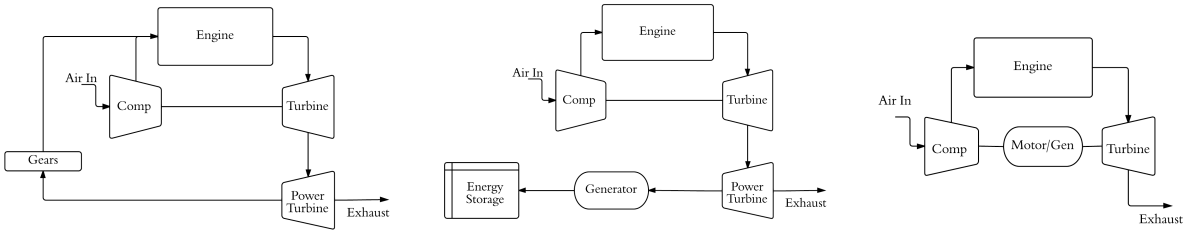

(a) Mechanical Turbocompounding (b) Turbogenerator (c) Electric Turbocharger

Figure 1: Turbocompounding layouts

Turbocompounding, in its various forms, has been shown to offer significant benefits in fuel consumption for large capacity engines. Sendyka and Soczowka [13] showed a 5-10% improvement in fuel consumption using a modelling approach applied to an electric turbocharger. This study also showed the best results were obtained when the engine was run at high load. Hopmann and Algrain [14] also showed the benefits of turbocompounding at full-load on a large-capacity engine. They reported up to 10% reduction in fuel consumption through a theoretical modelling approach, and up to 5% reduction in fuel consumption when real-world engine loads were analysed. Hountalas et al [15] compared mechanical turbocompounding to an electric turbocharger. The authors showed the mechanical setup to be the best configuration, delivering up to 4.5% reduction in fuel consumption at full-load on a large-capacity engine. The electric turbocharger produced almost no benefit at part-loads, but the authors showed the importance of matching the turbocharger to the new turbocompounded setup; if a revised turbocharger was used with increased efficiency, almost 3% reduction in fuel consumption was achieved.

1.1.4. Turbogenerator

Of the forms of turbocompounding discussed, the turbogenerator offers benefits to fuel consumption, high power density and small packaging requirements. Thompson et al [16] studied a turbogenerator on a 12-litre engine. The turbogenerator was run at a fixed speed and load point, but the authors showed that the power turbine speed was a key parameter to obtain maximum benefit from the turbogenerator and when the turbogenerator design was optimised, 9.1% improvement in fuel consumption compared to the baseline turbocharged engine was achieved. This highlights an additional benefit which the turbogenerator offers over mechanical turbocompounding; the power turbine speed can be controlled to optimise the efficiency at any running point. Robinson and Smith [17] reported the performance of a turbogenerator on a 4-cylinder spark ignition engine. The authors aimed to create useful electrical power from the turbine, but did not specifically investigate the ability of the turbogenerator to improve fuel efficiency. The results showed the turbogenerator could create up to 11kW of power at certain operating conditions, but this produced a reduction in fuel efficiency, highlighting the difficulty in balancing power turbine power with backpressure. When a power turbine of lower power output was used and carefully controlled, the fuel efficiency was shown to improve by up to 6% at one operating condition.

Papers which discuss the benefits of a turbogenerator on smaller-capacity engines are more limited. Wei et al. [18] used a turbogenerator fitted to a 1.8-litre spark-ignition engine, again at full-load. The authors noted the importance of choosing a power turbine flow capacity large enough to avoid high backpressure penalties, but they showed results in which little or no effect on fuel consumption is demonstrated. The turbine they used did not generate significant power as most of the engine's flow was bypassed around the power turbine. Michon and Johnstone [19] showed a turbogenerator used on a 2.0-litre normally-aspirated spark ignition engine, and suggested that up to 6% reduction in fuel consumption is possible. However, no evidence was presented to back up this claim, and the paper mainly concerned the power that can be generated from such a device rather than the fuel consumption benefits. Mamat et al. [20] studied the design of a low-pressure ratio turbine for a turbocompounding application on a 1.0-litre turbocharged spark-ignition engine. The authors showed potential benefits of up to 3% improvement in fuel consumption. No other

studies were found which analysed the effect of turbocompounding on a low-capacity diesel engine, though a previous study by Briggs et al. [21] has also shown that up to 3% reduction in fuel consumption can be achieved on a 2.4-litre turbocharged diesel engine.

The literature presented above shows that turbocompounding, and in particular, the turbogenerator concept can play a significant role in reducing fuel consumption in low-capacity turbocharged engines such as the one used in the Wrightbus diesel-electric hybrid bus, and the power generated can be easily integrated into the existing electrical energy storage system.

1.2. Hybrid Vehicles

The hybridisation of vehicles is one way in which bus operators have achieved low carbon emissions status. Hybrid drivetrains offer the potential to reduce greenhouse gas emissions, and in turn, fuel consumption by offering energy storage systems. Most often, this includes a system for storing energy created during braking (regenerative braking) and storing the energy of the ICE. This allows the ICE to be decoupled from the energy demanded by the vehicle, and therefore the ICE can be run at a more efficient combination of load and speed.

There are various types of drivetrain available for use on a diesel-electric platform. Wrightbus use a series-hybrid platform as shown in Figure 2. This configuration breaks the link between the engine and the wheels, with excess power from the engine being stored in a high voltage battery system.

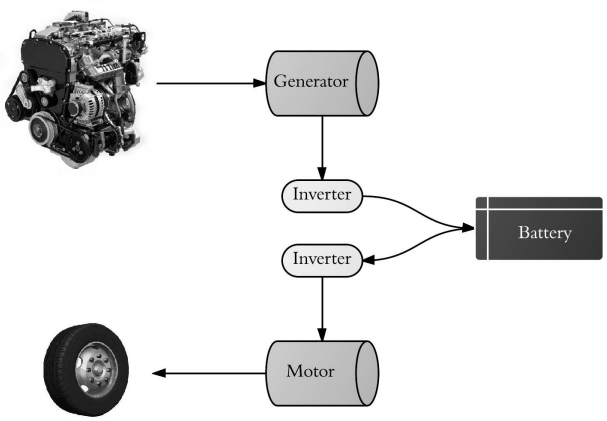

Figure 2: Series Hybrid Drivetrain

For vehicles such as buses whose drive cycle profile may include long periods of stop/start driving, acceleration and decelerations, a conventional bus operating with an ICE as the sole energy generator would operate its engine mainly at part-load and low speed, where the engine is least efficient. Therefore a series hybrid drivetrain can avoid this by using the batteries to power the vehicle when the performance of the engine alone would be sub-optimal.

Andersson [22] studied the modelling of hybrid buses. The model included components for the internal combustion engine and electric drive motors. The model in this paper was created using MATLAB/Simulink and contained modules for choosing different types of bus, drive cycles, component types and charging strategies.

Efficiency maps were supplied for the motors and ICE while the battery was modelled as a simple voltage source which varied with state of charge. As battery resistance varied with its temperature, battery losses were calculated, and included in the calculation for state of charge. No user control was allowed over specific engine components or the operation of the engine as a whole. The engine controller determined the most suitable speed and torque to run the engine at, based on the power requirement and the minimum achievable fuel consumption to obtain that power. Although not explicitly stated, it was assumed that the engine module contained a map of fuel consumption at all engine speed and torque points.

Berta et al. [23] outlined the development of a computational model to simulate the performance of hybrid buses. The model simulated the performance of a series hybrid drivetrain and was applied to various bus platforms ranging from small 20-passenger vehicles to larger 90-passenger buses. The model could be configured to run either in backward- or forward-facing modes and the author suggested that the former should be used to assess the energy balance of the vehicle, while the latter should be used to assess the performance and driveability of the bus as it used driver inputs to determine the vehicle's operation.

The author recognised the importance of the battery module in successfully simulating the bus and considerable validation was carried out on this aspect. Battery state of charge was calculated based on instantaneous battery current as a percentage of its rated current. Real-life drive cycles were used to accurately simulate the performance of the bus.

Simpson [24] developed a model of a Wrightbus series hybrid bus platform using MATLAB/Simulink. The model was split into three main components to model the drive cycle, engine and generator, and battery module. Within the model, various drive cycles could be selected by the user, and the developer enabled the engine to be changed independently from the vehicle. Individual components such as vehicle mass, auxiliary loads and road profile could be changed in a manner similar to that described by Andersson [22], but more control over the details of these components was possible.

Various battery charging strategies were also developed by Simpson [25] which enabled the hybrid bus to carry out either a load-following strategy or state of charge-following (SOC-following) strategy. A load-following strategy was one where the engine attempted to deliver most of the power demanded by the series hybrid platform, and the drive power was supplemented by the battery. In this mode, the engine control and drive motors were closely coupled to minimise energy storage. An SOC-following strategy was one where the engine was operated only to maintain battery SOC; the user controlled the amount of discharge within the battery before the engine was used to recharge it. In this mode, the engine and drive motors were completely separated and the drive power was supplied purely by the battery.

The battery management strategy involved a starting value for SOC (nominally 55%), and the user could determine the amount of discharge allowed (ΔSOC) before the battery was recharged from the engine/generator. The default values for ΔSOC was 5%. In this way, the user could determine the main parameters for the battery control strategy and influence the charging strategy and operation of the hybrid bus.

The model was extensively validated and was shown to closely match experimental data which the author obtained from bus testing. The most critical aspect of the model was shown to be the energy storage [24] and extensive calibration was undertaken to ensure correct prediction of SOC. The prediction of SOC over a drive cycle showed good agreement with experimental data. The full workings of the hybrid bus model are discussed in more detail in section 2.4.

Although hybrid technology reduces emissions and fuel consumption, there is still energy wasted due to the inherent inefficiency of the ICE. By combining hybridisation with exhaust energy recovery, significant improvements in efficiency may be achieved. This paper shows the benefits to be gained in fuel consumption, by close-coupled modelling and optimisation of the engine and the hybrid bus platform.

2. Methodology

2.1. Introduction

A modelling approach to waste energy recovery of a diesel-electric hybrid bus is presented, and the approach consisted of two separate modelling strands. The initial effort was spent on modelling the energy recovery system; a turbogenerator was installed on a fully-validated baseline model of the 2.4-litre diesel engine for the application described above, using *WAVE* 1-D engine modelling software. The validation process is described in section 2.2.

This turbogenerator model was then run across the full operating range of the engine in the hybrid bus and a modified brake specific fuel consumption (BSFC) map was produced which included the effect of energy recovery.

The modified BSFC map was then included in a QUB-developed Hybrid Powertrain Model (HPM), which accounted for the operation of the hybrid bus, including such factors as road profile, acceleration/deceleration and auxiliary loads on the bus such as air-conditioning. The HPM is described in section 2.4.

2.2. Baseline Engine Model

The engine used in the bus is a Ford Duratorq 2.4-litre, 4-cylinder, turbocharged diesel engine. The engine uses a common rail fuel injection system. The creation of the 2.4-litre diesel engine model is described in detail in [26]. In summary, an initial baseline model was created and validated against a wide range of cycle-averaged experimental data at a comprehensive matrix of operating conditions. A BSFC map for the engine was produced as shown in Figure 3. The position of minimum BSFC is shown and red contours represent high values of BSFC, while blue values represent lower values. It can be seen how the 'eye' of the BSFC map is towards the low-speed, high-load side of the map, and also how the map is relatively flat with only small variations in BSFC away from the optimum point.

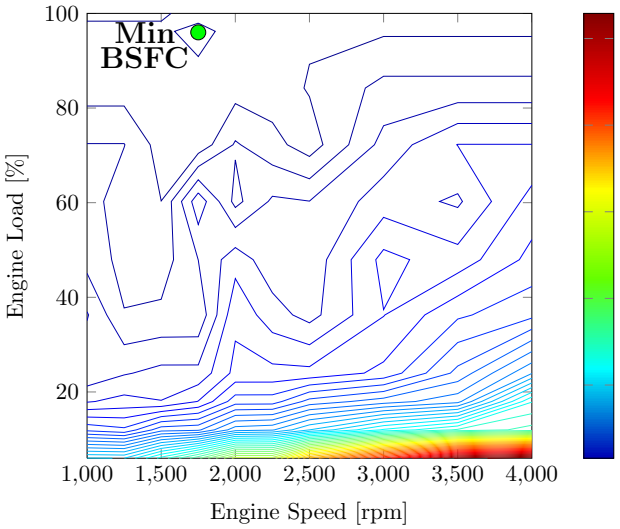

Figure 3: Baseline engine BSFC map

The model was also subsequently validated against crank angle-resolved, in-cylinder pressure at four common operating points as shown in Table 1. These operating points were obtained from a frequency analysis of four drive cycles over which the bus operates. The most commonly accessed speed and load points were thus obtained. This in-cylinder validation is shown at the four analysis points in Figure 4.

Table 1: SUMMARY OF VALIDATION POINTS.

Point	Engine Speed [rpm]	Load [%]
Pt1	1000	12
Pt2	1500	47
Pt3	2000	71
Pt4	2500	100

The model can be seen to have predicted peak cylinder pressure to within 3 bar (∼2.4%) of the measured data at full-load (Pt4), while at part-load the comparison was even more favourable in terms of peak cylinder pressure. Some slight misalignment in the location of peak pressure existed in all models, but generally the

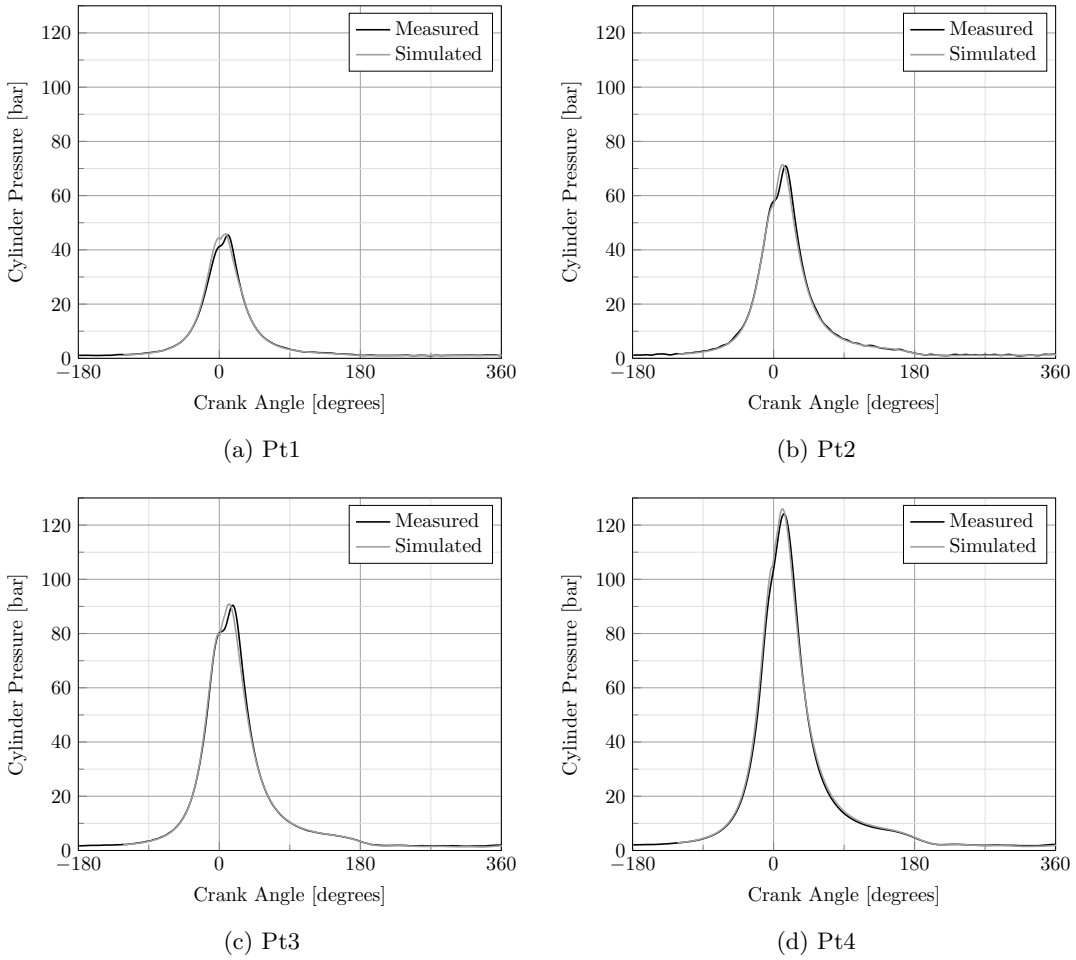

(a) Pt1

(b) Pt2

(c) Pt3

(d) Pt4

Figure 4: In-cylinder validation: crank angle-resolved pressure comparison

error was small and the combustion model used performed well. Other validation data for the baseline engine can be seen in Tables 2 and 3.

Some small errors occurred in IMEP_{net} at full-load (Pt4 in Table 3) due to small fluctuations which were present in the experimental pressure trace of the pumping loop, but the $\text{IMEP}_{\text{gross}}$ comparison was good. Pressures in the inlet and exhaust manifold were also predicted well with the model, though some small errors in intake and exhaust pressure occurred in the part-load cases due to difficulties in modelling and controlling high-pressure EGR flow. Temperatures in the intake and exhaust manifolds were also predicted well.

2.3. Turbogenerator Model

The validated baseline model was then extended to include a turbogenerator. This involved the addition of a power turbine downstream of, and in series with, the turbocharger turbine as described in previous studies by the author [26]. Three different sizes of turbogenerator were created with different rated power output: 4.6kW, 7.0kW and 9.3kW at full engine load. These devices represent 6.6%, 10.5% and 13.9% respectively of the engine's power output at the turbogenerator design point (67.5kW at Pt4). The power turbines were created using a generic turbine map which provided a suitable combination of pressure ratio, mass flow rate and efficiency. The maps were subsequently scaled in mass flow, in keeping with literature [27], to provide a suitable range of mass flow rates for the engine used in this project. The power output of each

Table 2: VALIDATION PARAMETERS AT PT1 AND PT2.

		Pt1		Pt2	
Parameter	Unit	Measured	Simulated	Measured	Simulated
$IMEP_{net}$	[bar]	2.85	2.74	8.95	8.84
P_{intake}	[bar]	1.02	1.01	1.25	1.16
$P_{exhaust}$	[bar]	1.07	1.02	1.39	1.18
T_{intake}	[K]	297.5	350.6	300.1	306.2
$T_{exhaust}$	[K]	485.3	500.3	714.3	705.6
BSFC Error	[%]	–	2.26	–	1.31

Table 3: VALIDATION PARAMETERS AT PT3 AND PT4.

		Pt3		Pt4	
Parameter	Unit	Measured	Simulated	Measured	Simulated
$IIMEP_{net}$	[bar]	13.31	13.06	17.52	18.15
P_{intake}	[bar]	1.71	1.68	2.12	2.18
$P_{exhaust}$	[bar]	1.75	1.56	2.01	1.90
T_{intake}	[K]	300.6	314.0	311.9	325.7
$T_{exhaust}$	[K]	788.2	804.9	871.6	875.4
BSFC Error	[%]	–	0.59	–	0.07

turbogenerator was determined by the mass flow scaling factor used in each turbine map. For the 4.6kW, 7.0kW and 9.3kW turbogenerators, the mass flow scaling factors were 0.8, 1.0 and 1.2 respectively. The map of the 7.0kW turbogenerator turbine is shown in Figure 5. The mass flow rate was subsequently scaled as described above to produce the maps for the other two turbogenerators.

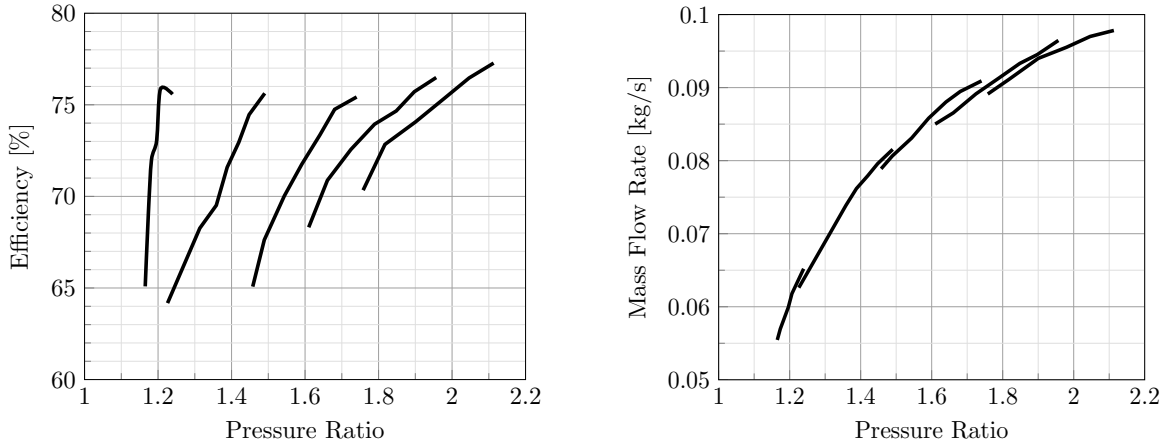

(a) Efficiency v Pressure Ratio

(b) Mass Flow v Pressure Ratio

Figure 5: Turbogenerator turbine maps

The speed of the power turbine was controlled between 40,000rpm and 120,000rpm to ensure the turbine operated at the highest efficiency possible at each engine speed and load point. In reality, altering the speed

of the turbogenerator turbine would be performed by the power electronics of the turbogenerator, which would limit the speed of the device according to the operating point of the engine. The model was controlled to maintain AFR and torque at the same levels as the baseline model.

This turbogenerator model was then run across the full operating range of the engine to obtain a modified BSFC map, and a corresponding map of turbogenerator power at every load and speed point. In doing so, the engine's torque and AFR were maintained as near as possible to the values of the baseline model so as not to impact driver load demand or emissions.

2.4. Hybrid Powertrain Model

2.4.1. Introduction

In analysing the impact of waste energy recovery on a hybrid bus, the QUB-developed Hybrid Powertrain Model (HPM) based on work by Simpson [24] was used. This model took the output from the engine model in the form of a modified BSFC map and a corresponding map of turbogenerator power at every operating point. It then used drive-cycle data to analyse the performance of the bus in real-world conditions including road loads, auxiliary power loads, vehicle weight etc. The drive-cycle used in this work was the Route 159 London inner-city drive-cycle. The HPM is a backward-facing vehicle model comprising of three main sections: drive cycle data, engine-generator (genset), and a battery module. This ensures a high level of detail can be controlled in in each system of the hybrid bus.

2.4.2. Hybrid Powertrain Model Structure

The basic schematic layout of the HPM is shown in Figure 6. The drive cycle section of the model loads various drive cycles and obtains data such as road profile, acceleration and deceleration periods, elevation and vehicle speed. The user can also supply information pertaining to the auxiliary loads on the vehicle. This includes the power required by the cabin air-conditioning, battery compartment air-conditioning, electrical lighting and other electrical loads on the vehicle. The output from the drive cycle block comprises the vehicle's velocity and distance travelled, along with the power required from the engine and power demanded by the auxiliary loads.

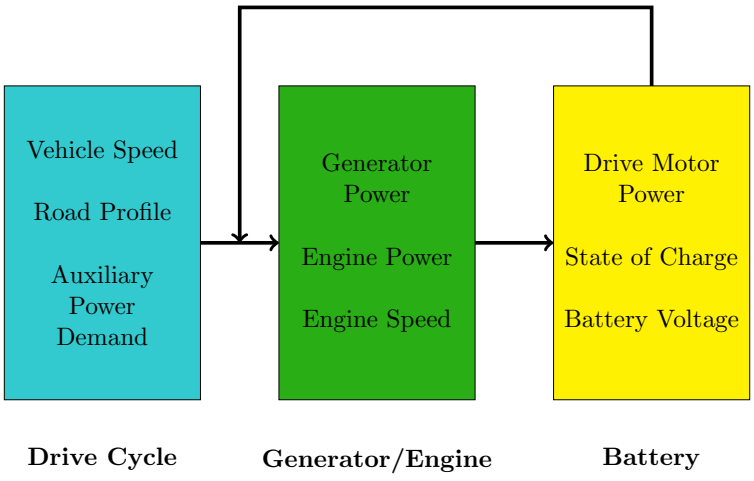

Figure 6: Hybrid Powertrain Model configuration [24]

The generator/engine module uses the vehicle's velocity along with various battery properties such as state of charge (SOC) and voltage to calculate the power required to drive the vehicle. It supplies this data to a vehicle control unit which determines the operating point of the generator, and an ECU then controls how the engine should operate to achieve this demand. The efficiencies of motors and generators are taken

into account in the model as well as generator inertia, which affects spin-up and ramp-down rates. The fuel used is determined via a lookup table of BSFC as described above.

The battery module is where calculations relating to battery SOC take place. SOC is largely based on the generator, motor and connector efficiencies, along with battery resistance. To produce valid comparisons between tests, a correction must be applied to account for differences between initial and final SOC. The calculation procedure for corrected SOC follows that described in [28]. Firstly, the net energy change (NEC) of the battery is calculated based on the initial and final SOC (in Ampere-hours) and nominal voltage as in Equation 1. A conversion factor of 3600 is included to convert Ampere-hours to Ampere-seconds. For runs which have $SOC_{final} < SOC_{initial}$, this will produce a negative value for NEC.

$$NEC = [SOC_{final} - SOC_{initial}] \times V_{system} \times 3600 \tag{1}$$

The total fuel energy supplied to the vehicle is known from Equation 2, where CV_{fuel} is the calorific value of the fuel in J/kg, and m_{fuel} is the mass of fuel burned in units of kg. This represents the total energy available for use in the engine before the fuel is burnt.

$$E_{fuel} = CV_{fuel} \times m_{fuel} \tag{2}$$

The total cycle energy is then calculated from Equation 3. This shows the amount of energy needed to return the battery to the initial state of charge.

$$E_{cycle} = E_{fuel} - NEC \tag{3}$$

If $1\% \leq \frac{NEC}{E_{cycle}} \leq 5\%$, the test is deemed to be valid and the correction shown in Equation 4 is applied to the final value of SOC to calculate the extra fuel which would be used to return the SOC of the battery to the initial value.

$$m_{extrafuel} = \left(\frac{\overline{BSFC}}{\eta_{total}}\right)\left(-\frac{NEC}{3.6 \times 10^6}\right) \tag{4}$$

where $\overline{BSFC}$ is the mean value of BSFC over the drive cycle and η_{total} represents the combined efficiency of the electrical system, including generator, batteries and heat losses. This correction procedure is implemented within the battery module of the HPM and is used to calculate a corrected fuel consumption figure in miles per gallon.

For this paper, the HPM was operated in a load-following strategy. This meant that the vehicle demanded a certain amount of power from the generator, which in turn operated the batteries and engine to satisfy this demand. This meant as little of the engine's power as possible was stored in the battery, but if an excess of power was created, it could be used to charge the battery. The model also had inbuilt SOC limits, which the user could control. For example, the initial SOC could be varied along with the target SOC, which the genset would aim to maintain. The amount of discharge could also be controlled, i.e. the model would allow the battery to discharge by a certain percentage before it was recharged by the engine.

The operation of the genset was based on a user-specified input profile which related the power demand of the vehicle to the power supplied by the engine. At very low power demands, the generator did not operate, and instead the power was delivered by the battery alone. Above a threshold value of power demand, the engine was used as the primary power source. The relationship between demand and supply could be controlled and modified to suit a particular application. For the bus used in this work, a generator profile was supplied by the bus manufacturer.

2.4.3. Modifications for Energy Recovery

To accommodate energy recovery in the HPM, changes were made to the genset module. The power created by the turbogenerator was connected to the 24V auxiliary power circuit, and the turbogenerator power was therefore used to satisfy the demand of the auxiliary loads described above, thus reducing the amount of power demanded of the engine for this purpose. The engine speed and torque was used to determine the turbogenerator power based on the power map supplied from the engine model. Rate limits

were applied to this value of power to account for the inertia of the turbogenerator, and the auxiliary power demand was then reduced by this value of turbogenerator power. The reduced auxiliary power signal was then fed to the ECU, VCU and engine as before. Throughout this work, the auxiliary load demanded from the bus was set at 12kW, a value typically used in the vehicle. The power generated by the turbogenerator was therefore always lower than the auxiliary load demand, even at peak turbogenerator power output.

This simple method of integrating energy recovery in the HPM allowed the distribution of power to be monitored throughout the drive cycle, and by reducing the auxiliary load requirement, the effect on battery SOC could be observed.

3. Discussion of Results

3.1. Turbogenerator Results

The three turbogenerator models were run at the same four steady-state load/speed points at which the baseline engine was validated (see Table 1 above). These four points and the corresponding improvement are shown in Figure 7.

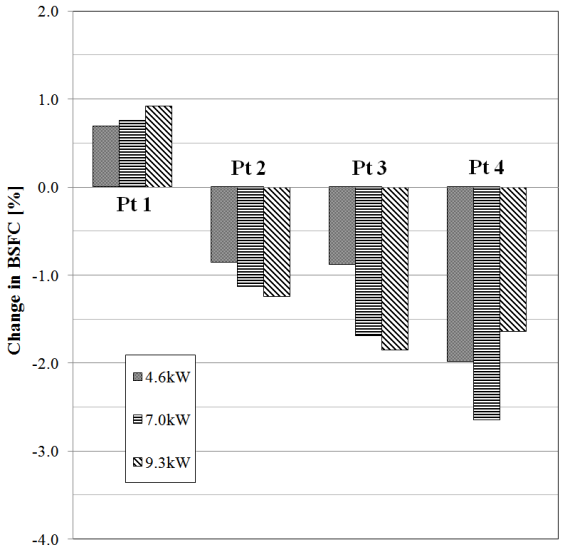

Figure 7: BSFC improvement at four steady-state validation points

This steady-state analysis shows that the 7.0kW device provided the most benefit at full-load (approximately 2.6% reduction in BSFC at Pt4), while at part-load (Pt2 and Pt3), the 9.3kW device provided the most benefit to BSFC. At low-load none of the turbogenerator devices produced a benefit to BSFC, mainly due to the low levels of exhaust energy available at this condition, along with the associated impact on backpressure that the turbogenerator produced. The 4.6kW device showed the least benefit to BSFC as the power it creates at part-load conditions is low.

Figure 8a shows the effect each turbogenerator had on backpressure. It is clear from this figure how backpressure increased to a large extent at Pt4. The 9.3kW turbogenerator produced an increase in backpressure of almost 130%. This equates to an increase in the turbocharger turbine inlet pressure of almost 2.4bar. Comparing this to Figure 8b it can be seen how the 9.3kW turbogenerator produces almost 14% of the power produced by the engine. Clearly, with such a large increase in backpressure this represents an insufficienct power output from this device. This explains why the change in BSFC in Figure 7 was lower than the 7.0kW turbogenerator which, at Pt4, offers over 10% of the engine's power output, with a corresponding increase in backpressure of 82%. This represents an increase in turbocharger turbine inlet pressure of 1.5bar. There is therefore a clear balance between the power produced by the turbogenerator

and the increased backpressure it causes. This increase in backpressure, when it increases above a certain point, causes an unacceptable increase in pumping work from the engine, and therefore is not offset by the power produced by the turbogenerator.

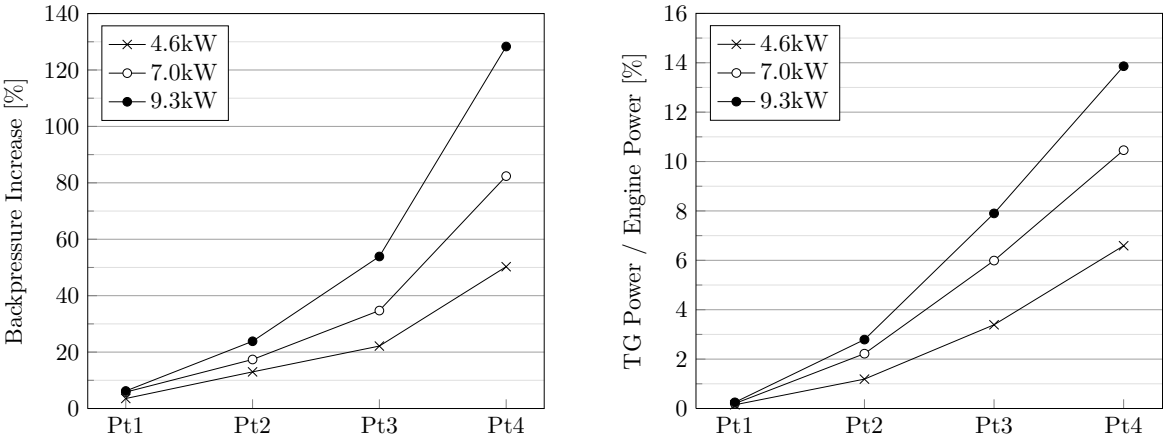

(a) Backpressure caused by turbogenerator

(b) Turbogenerator power

Figure 8: Backpressure effects

This implies that the operation of the turbogenerator, and the optimum size of device, is therefore linked closely to the operation of the bus, i.e. if the engine accesses more part-load conditions, the size of turbogenerator required will be different than if the bus mostly operates at full-load. The devices presented here were designed to operate at both full- and part-load conditions.

3.2. Hybrid Powertrain Model Results

The turbogenerators were simulated in the HPM to analyse the performance of the devices on the bus over the Route 159 drive cycle. The initial effects on fuel consumption are shown in Table 4.

Table 4: SUMMARY OF INITIAL ROUTE 159 DRIVE CYCLE RESULTS.

Configuration	Effect on Fuel Consumption
Baseline Engine	–
4.6kW TG	-1.4%
7.0kW TG	-2.4%
9.3kW TG	+0.4%

This data shows the 7.0kW TG performed best over the Route 159 drive cycle, offering a 2.4% reduction in fuel consumption. This agrees well with the steady-state results shown in section 3.1, and shows the TG can reduce fuel consumption over real drive cycles. However, the 9.3kW device had a small *negative* impact on fuel consumption. This is due to the nature of the operating profile of the bus; because the bus operates at engine points where the 9.3kW device offers no improvement in BSFC, it is switched off at more points than the 7.0kW device. Due to the inertia of the turbogenerator, and the effect this has on spin-up rates, the 9.3kW device performed less well than the 7.0kW device which was able deliver power at more of the operating points of the engine.

The changes to the bus operation produced by the turbogenerator can be seen in the state of charge plot in Figure 9. This shows how the 7.0kW device allowed the battery SOC to remain higher for longer than both the baseline model and the other two turbogenerators, and when the battery reaches its minimum

allowable SOC (50%) the 7.0kW turbogenerator also charges the battery quicker than the baseline model. This is due to the reduction in auxiliary power demand as detailed above and all three turbogenerators perform similarly during the charging phase. The turbogenerators reduce the drain on the batteries, so SOC stays higher, and the battery requires less energy from the engine to charge. For the 7.0kW turbogenerator, the charge periods reduced from 333 seconds to 308 seconds (a 7.5% reduction in charging time), as can be seen in Figure 9.

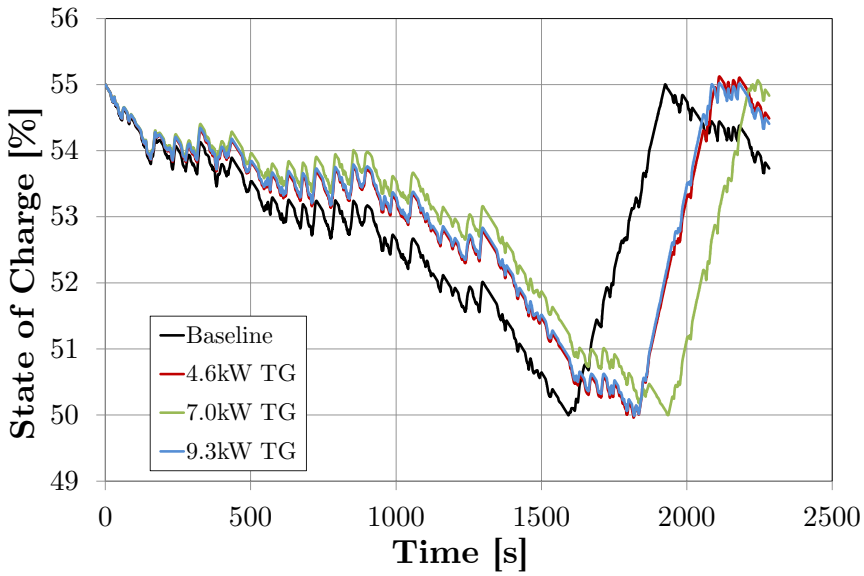

Figure 9: SOC variation with turbogenerator power output

3.3. Genset Modification

The initial results in section 3.2 prove that the turbogenerator was able to reduce fuel consumption over a drive cycle. However, to extract the maximum benefit from the device, the operation of the bus' generator and engine (genset) was investigated. The genset was controlled by a user-input profile which was supplied from the manufacturer. This determined the power that the generator requests from the engine based on the power required by the vehicle, and resulted in the engine operating frequently at approximately 70% load at 1800rpm as shown by point A on the BSFC map in Figure 10.

The reasons for operating away from the point of minimum BSFC are mainly due to battery usage and life. By running at a lower power point, aggressive charging is avoided and hence heat losses are minimised. A study by Johri [29] also suggested this is likely to happen for similar reasons, but also to avoid spending undue amounts of time at idle speeds due to frequent charging periods. This is less of a concern in this project as the load-following nature of the bus control strategy means it spends little time at idle while the bus is in motion.

It can also be seen how the point of minimum BSFC moves to a higher engine speed and a slightly higher engine load when using the 7.0kW turbogenerator. This is closer to the design point of the turbogenerator (Pt4). Figure 10 can be compared to Figure 3 for reference, and it can be seen that only subtle differences are apparent when the turbogenerator is applied. Clearly, Point A represents an operating condition that is far away from its optimum efficiency setting.

The efficiencies of the turbocharger compressor and turbine and brake thermal efficiency at point A are shown in Table 5. The efficiency of the compressor was lower than was desirable, and so the engine model results were analysed and the genset power levels set in such a way as to run the engine at a more efficient operating point, with a lower baseline BSFC. As is typical of diesel engines, the most efficient

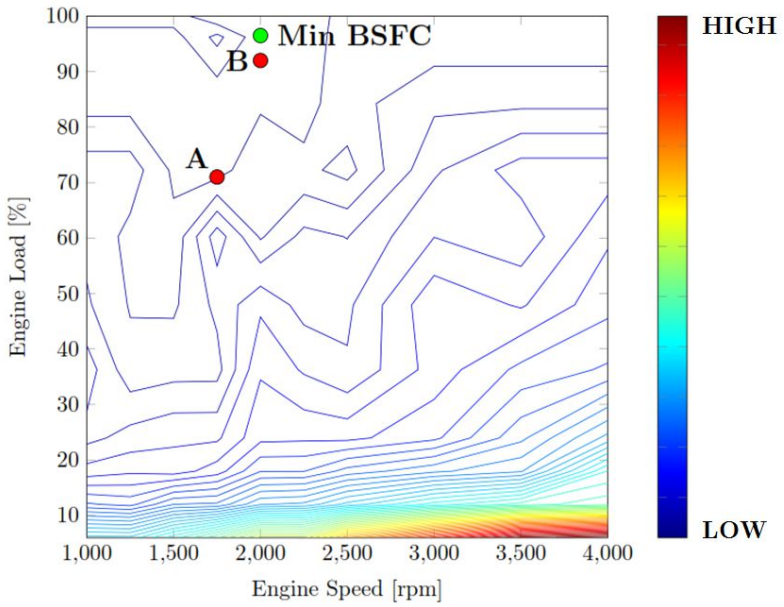

Figure 10: Genset operating points on turbogenerated engine BSFC map

running points are at high-load and low-speed, and in this analysis, the genset could be set at 92% load and 2000rpm in order to run at a point close to the minimum BSFC on the engine map, as shown by point B in Figure 10. The HPM determines the load setting of the engine based on the generator speed and engine power required. This means that operating exactly at the point of minimum BSFC was not possible since a suitable combination of load and speed could not be obtained to give the required power output. Operating at Point B therefore represents the best compromise in obtaining a running point close to the point of the engine's maximum efficiency. This resulted in the efficiencies shown in Table 6, showing an improvement in all parameters.

Table 5: EFFICIENCIES AT 70% ENGINE LOAD, 1800RPM (Pt A).

Property	Efficiency [%]
Turbocharger Compressor	71.8
Turbocharger Turbine	73.3
Brake Thermal	40.3

Table 6: EFFICIENCIES AT 92% ENGINE LOAD, 2000RPM (Pt B).

Property	Efficiency [%]
Turbocharger Compressor	74.9
Turbocharger Turbine	74.1
Brake Thermal	40.9

With this new genset control strategy in place, the original baseline engine model was re-run to obtain a new optimised baseline fuel consumption figure, which showed an increase of 2.9% over the original baseline

model. Running the turbogenerator on this configuration produced results as shown in Table 7.

Table 7: FUEL CONSUMPTION RESULTS WITH OPTIMISED GENSET.

Configuration	Change	Change over original baseline
Optimised Baseline	–	-2.9%
4.6kW TG	-2.1%	-5.1%
7.0kW TG	-3.0%	-6.0%
9.3kW TG	-2.1%	-5.1%

Clearly, by optimising the control strategy of the generator, all the models showed an improved reduction in fuel consumption. The 2.9% improvement in baseline occurred due to operating at a more efficient engine point, which highlights the benefit of closely integrating the modelling of the engine, energy recovery and hybrid vehicle. Table 7 also shows that the performance of the turbogenerators is more closely matched in this optimised configuration. The 7.0kW device still performs best and produced a 3.0% improvement in fuel consumption over the optimised baseline model. When compared to the original baseline model, this represents a 6.0% reduction in fuel consumption by using the 7.0kW turbogenerator.

There may be operational reasons why the current genset strategy involves running the engine at 40kW rather than 61kW. For example, NVH (noise, vibration and harshness) factors, which impact passenger comfort, may mean that running the engine at this higher power point may be unacceptable. Also, running at a higher engine power may adversely impact battery life and usage. The impact that running the engine at a higher power point has on these factors has not been investigated in this study, and could form the basis of future work. However, the results presented in Table 7 show the benefits of closely-coupled engine/vehicle modelling, in that changes to the operation of the vehicle may be suggested.

3.4. Payback Analysis

To calculate the value of the turbogenerator for bus operators, the current fuel price in the UK was used to make some estimates of the financial savings made possible by recovering waste energy. According to the UK Department for Transport [30], 46,300 buses were on the road in the UK in 2011. Collectively they covered 1.15 billion miles (1.85 billion km). This equates to an average of almost 25,000 miles (40,233 km) per vehicle per year.

Assuming an average fuel consumption of 4 miles per gallon (58.8 litres/100km) [31], this equates to over £41,000 of fuel per bus per year at current market rates. Therefore, a turbogenerator that could reduce this by 3% would reduce fuel costs by over £1200 per bus per year.

Immediately, it is apparent how much the turbogenerator is worth in financial terms. Most bus operators want to recover their costs over five years [32], in which case the device would have to be priced around £6000 to make it financially viable. The figures presented above for fuel usage are perhaps conservative, since they represent a country-wide average of fuel usage for a variety of vehicle types; it is likely that inner city double deck buses will use much more fuel than that shown above, and consequently the price of the turbogenerator could be higher and still be commercially attractive for operators.

Whilst this analysis does not include any installation costs associated with the turbogenerator, the aim must be to recover more energy and balance the cost of this device against the benefits it brings in terms of fuel consumption. For bus operators, all improvements in fuel consumption by recovering otherwise wasted energy contribute to the effort to reduce emissions and achieve low-carbon vehicle status.

4. Conclusions

The work reported in this paper studied the effect of recovering wasted energy on the exhaust line of a diesel-electric hybrid bus. A 1-D engine model was created and validated against experimental data and a turbogenerator was subsequently simulated in the model to recover the waste exhaust energy.

A parametric study showed that the optimum size of turbogenerator for use on a 2.4-litre turbocharged diesel engine is a device with a rated power of 7.0kW at full engine load (6.8% of the engine's rated power output). This produced a 2.6% reduction in steady-state BSFC at full engine load, and up to 2% reduction in BSFC at part-load conditions. This study highlighted the importance of matching the size of turbogenerator to suit the exhaust mass flow of the vehicle to avoid creating unacceptable increases in backpressure.

The importance of analysing the device over a drive cycle was evident from the differences produced at various engine load and speed conditions. To this end, a Hybrid Powertrain Model (HPM) was used in conjunction with the 1-D engine model, and the devices were analysed over the Route 159 London bus drive-cycle. This work showed that over the drive cycle, up to 2.4% reduction in fuel consumption was observed.

If the bus' generator control strategy could be optimised and applied to both the baseline and turbogenerator models,the optimised baseline model improved fuel consumption by 2.9%, and the optimised turbogenerator model improved fuel consumption by a further 3.0%, representing a 6.0% improvement over the original baseline model.

A value analysis also showed the financial benefits the turbogenerator could bring if this 3% reduction in fuel consumption is realised. An average saving of £1200 per year per bus means, as bus manufacturers want to recoup their costs over five years, the device would need to be priced below £6000 to be financially viable for operators.

Acknowledgement

The authors would like to thank the UK Technology Strategy Board and Invest Northern Ireland for part-funding the work, and Wrightbus Ltd, Ricardo Ltd, and Revolve Technologies Ltd for their technical contributions and the supply of test data used to validate the models.

Nomenclature

Abbreviations

AFR	Air-to-fuel Ratio
BSFC	Brake Specific Fuel Consumption
CAFE	Corporate Average Fuel Economy
CO	Carbon Monoxide
CV	Calorific Value
ECU	Engine Control Unit
EVO	Exhaust Valve Opening
HC	Hydrocarbons
HPM	Hybrid Powertrain Model
ICE	Internal Combustion Engine
IVC	Intake Valve Closing
IMEP	Indicated Mean Effective Pressure
NEC	Net Energy Change
NO_X	Oxides of Nitrogen
NVH	Noise, Vibration and Harshness
ORC	Organic Rankine Cycle
PM	Particulate Matter
QUB	Queen's University Belfast
SOC	State of Charge
TEG	Thermoelectric Generator
TG	Turbogenerator
VCU	Vehicle Control Unit

Symbols

E	Energy	Joules
m	Mass	kg
P	Pressure	bar
T	Temperature	K
V	Voltage	Volts
η	Efficiency	-

Subscripts

cycle	Full cycle energy
exhaust	Located in exhaust manifold
gross	Gross IMEP (Does not include PMEP)
intake	Located in intake manifold
net	Net IMEP (Includes PMEP)

References

[1] European Union, Reduction of pollutant emissions from light vehicles, Online, Available: goo.gl/EllVi [Accessed: 27 March 2013].

[2] National Highway Traffic Safety Administration, Corporate Average Fuel Economy (CAFE) Standards, Online, available: www.nhtsa.gov/fuel-economy/ [Accessed: 10 August 2013].

[3] A. Obieglo, J. Ringler, M. Seifert, W. Hall, Future efficiency dynamics with heat recovery, in: Directions in Engine-Efficiency and Emissions Research, Technical Session 5: High Efficiency Engine Technologies, Dearborn, USA, 2009.

[4] J. Lopes, R. Douglas, G. McCullough, R. O'Shaughnessy, A. Hanna, C. Rouaud, R. Seaman, Review of rankine cycle systems components for hybrid engines waste heat recovery, in: SAE Commercial Vehicles Congress, Rosemont, USA, SAE Paper Number: 2012-01-1942, 2012.

[5] K. K. Srinivasan, P. J. Mago, S. R. Krishnan, Analysis of exhaust waste heat recovery from a dual fuel low temperature combustion engine using an organic rankine cycle, Energy 35 (6) (2010) 2387 – 2399. doi:10.1016/j.energy.2010.02.018.

[6] C. R. Nelson, High engine efficiency at 2010 emissions, in: Directions in Engine-Efficiency and Emissions Research, Technical Session 3: Diesel Engine Development, Chicago, USA, 2005.

[7] A. Domingues, H. Santos, M. Costa, Analysis of vehicle exhaust waste heat recovery potential using a Rankine cycle, Energy 49 (2013) 71 – 85.

[8] D. Crane, Potential thermoelectric application in diesel engine, in: 9th Diesel Engine Emissions Reduction (DEER) Conference, Session 4: Waste Heat Utilization, Newport, USA, 2003.

[9] D. Rowe, Thermoelectric waste heat recovery as a renewable energy source, International Journal of Innovations in Energy Systems and Power 1 (1) (2006) 13–23.

[10] J. Fairbanks, Thermoelectric applications in vehicles status 2008, in: 6th European Conference of Thermoelectrics, Session PL-01, Paris, France, 2008.

[11] X. Gou, S. Yang, H. Xiao, Q. Ou, A dynamic model for thermoelectric generator applied in waste heat recovery, Energy 52 (2013) 201 – 209.

[12] H. Hiereth, P. Prenninger, Charging the Internal Combustion Engine, 1st Edition, Springer, New York, p. 60, 2007.

[13] B. Sendyka, J. Soczówka, Recovery of exhaust gases energy by means of turbocompound, in: 6th Int. Symp. Diagnostics and Modeling of Combustion In Internal Combustion Engines, Yokohama, Japan, 2004, pp. 99–103.

[14] U. Hopmann, M. Algrain, Diesel engine electric turbo compound technology, in: Future Transportation Technology Conference & Exposition, SAE Paper Number: 2003-01-2294, Costa Mesa, USA, 2003.

[15] D. Hountalas, C. Katsanos, V. Lamaris, Recovering energy for the diesel engine exhaust using mechanical and electrical turbocompounding, in: Soc. Automotive Engineers Int. World Congr., Detroit, USA, 2007, SAE Paper Number 2007-01-1563.

[16] I. Thompson, S. Spence, C. McCartan, D. Thornhill, J. Talbot-Weiss, The technical merits of turbogenerating shown through the design, validation and implementation of a 1 dimensional engine model, International Journal of Engine Research (2012) doi:10.1177/1468087412458383.

[17] S. Robinson, L. Smith, Concept for exhaust energy recovery using a turbine electrical generator on a turbocharged spark ignition engine, in: Ricardo European Conference, Ludwigsburg, Germany, Paper Number 3, 2011.

[18] W. Wei, W. Zhuge, Y. Zhang, H. Yongsheng, Comparative study on electric turbo-compounding systems for gasoline engine exhaust energy recovery, in: ASME Turbo Expo 2010: Power for Land, Sea, and Air, Glasgow, UK, 2010, pp. 531–539, Paper Number GT2010-23204.

[19] M. Michon, G. Johnstone, Vehicle exhuast gas energy recovery using an integrated turbo-generator, in: 3rd Braunschweig Symposium, Braunschweig, Germany, 2006, pp. 94–110.

[20] A. M. I. Mamat, M. H. Padzillah, A. Romagnoli, R. F. Martinez-Botas, A high-performance low pressure ratio turbine for engine electric turbocompounding applications, in: ASME TurboEXPO 2011, Vancouver, Canada, 2011, GT-2011-45541.
[21] I. Briggs, G. McCullough, S. Spence, R. Douglas, R. O'Shaughnessy, A. Hanna, C. Rouaud, R. Seaman, A parametric study of an exhaust recovery turbogenerator on a diesel-electric hybrid bus, in: ASME TurboEXPO, San Antonio, TX, USA, 2013, Paper Number: GT2013-94492.
[22] C. Andersson, Observations on electric hybrid bus design, Master's thesis, Lund University (2001).
[23] G. L. Berta, E. Durelli, I. Nymann, Simulation models for hybrid buses, IMechE, Part D: Journal of Automobile Engineering 212 (1) (1998) 59–72.
[24] A. Simpson, R. Fleck, R. Kee, R. Douglas, D. Steele, A. Hanna, B. Maybin, Development of a Heavy Duty Hybrid Vehicle Model, SAE Commercial Vehicles Congress, Rosemont, USA, SAE Paper Number 2009-01-2933.
[25] A. Simpson, Hybrid Powertrain Modelling for Drive Cycle Optimisation, PhD Thesis, School of Mech. and Aerospace Eng., Queen's University Belfast (2010).
[26] I. Briggs, G. McCullough, S. Spence, R. Douglas, R. O'Shaughnessy, A. Hanna, C. Rouaud, R. Seaman, Waste heat recovery on a diesel-electric hybrid bus using a turbogenerator, in: SAE Commercial Vehicles Congr., Rosemont, USA, 2012, SAE Technical Paper 2012-01-1945.
[27] N. Karamanis, R. F. Martinez-Botas, Mixed-flow turbines for automotive turbochargers: Steady and unsteady performance, International Journal of Engine Research 3 (3) (2002) 127–138.
[28] Department for Transport, Vehicle Accreditation Requirements: Low Carbon Emission Buses, Online, available: www.lowcvp.org.uk/lceb/testing/procedures.asp [Accessed: 26 Mar. 2013].
[29] R. Johri, Z. Filipi, Low-Cost Pathway to Ultra Efficienct City Car: Series Hydraulic Hybrid System with Optimized Supervisory Control, SAE Int. Journal of Engines 2 (2) (2009) 505–520.
[30] Department for Transport, Annual Bus Statistics 2010/11, Online, Available: goo.gl/DkAaVs [Accessed: 23 Apr. 2013].
[31] Rogue Energy LLC, Advanced Clean Tech Batteries for Transit Busses, Online, Available: goo.gl/8HXGv [Accessed: 24 Apr. 2013].
[32] B. Maybin, Engineering Director, Wrightbus Ltd., Personal Communication, 25th April 2013.